

VHF profiler observations of winds and waves in the troposphere during the Darwin Area Wave Experiment (DAWEX)

R. A. Vincent, A. MacKinnon, and I. M. Reid

Department of Physics, University of Adelaide, Adelaide, South Australia

M. J. Alexander

Colorado Research Associates, Boulder, Colorado, USA

Received 1 March 2004; revised 26 May 2004; accepted 2 June 2004; published 11 August 2004.

[1] A VHF atmospheric radar (wind profiler) was used to study tropospheric winds during the Darwin Area Wave Experiment (DAWEX). The profiler, which operated at a frequency of 54.1 MHz, was located at Pirlangimpi (Garden Point) (11.4°S, 130.5°E) on the Tiwi Islands. Observations were made regularly up to heights near 8 km, with maximum heights occurring when convective activity was strongest. Mean winds observed between October and December 2001 are in good agreement with conditions that prevailed across northern Australia during this period. During the first two intensive observation periods (IOP) during October and November, the zonal and meridional wind components were westward and northward, respectively, with stronger values in November. By the time of IOP3 in mid-December, the zonal flow was eastward, a pattern that is typical of the Australian monsoon. Fluctuations in the three wind components for periods less than 3 hours are analyzed for IOP2 in November, when strong convective storms (“Hectors”) occurred on all afternoons over the Tiwi Islands. The fluctuations, which are ascribed to convectively generated gravity waves, show a correspondingly strong diurnal cycle, with horizontal wind variances peaking between 8 and 12 m²s⁻² in the early afternoon in the lower troposphere. Variances are only ~2 m²s⁻² in the early morning hours. A power spectral analysis shows that oscillations with ground-based periods between 8 and 17 min are especially prominent during Hector events. The profiler observations are compared with a numerical model study of gravity wave generation by convection on 17 November 2001. There is a satisfactory degree of agreement between the behavior of the model and profiler oscillations, both as a function of height and time.

INDEX TERMS: 3384 Meteorology and Atmospheric Dynamics: Waves and tides; 3314 Meteorology and Atmospheric Dynamics: Convective processes; 3307 Meteorology and Atmospheric Dynamics: Boundary layer processes; 3374 Meteorology and Atmospheric Dynamics: Tropical meteorology;
KEYWORDS: gravity waves, convection, VHF radar

Citation: Vincent, R. A., A. MacKinnon, I. M. Reid, and M. J. Alexander (2004), VHF profiler observations of winds and waves in the troposphere during the Darwin Area Wave Experiment (DAWEX), *J. Geophys. Res.*, 109, D20S02, doi:10.1029/2004JD004714.

1. Introduction

[2] The Darwin Area Wave Experiment (DAWEX) was designed to study the generation of gravity waves by convection and their subsequent propagation into the middle atmosphere and ionosphere. The focus of DAWEX was on the so-called “Hector” phenomena, which are intense convective events that occur on a diurnal basis during the premonsoon season over the Tiwi Islands north of Darwin, Australia. Three intensive observational campaigns (IOPs) were conducted between October and December 2001 in order to investigate

gravity wave generation by Hector thunderstorms and other convection in the vicinity of Darwin. For more information about the motivation for DAWEX and the instruments involved, the reader is referred to *Hamilton and Vincent* [2000] and K. Hamilton et al. (The DAWEX field campaign to study gravity wave generation and propagation, submitted to *Journal of Geophysical Research*, 2004, hereinafter referred to as Hamilton et al., submitted manuscript, 2004).

[3] Hector storms occur during the monsoon break flow characterized by deep subtropical easterly (westward) flow with a moderate maximum velocity near 3 km height [*Keenan et al.*, 2000]. The deep convective storms are forced along sea breeze fronts, and their orientation is determined by the low-level shear.

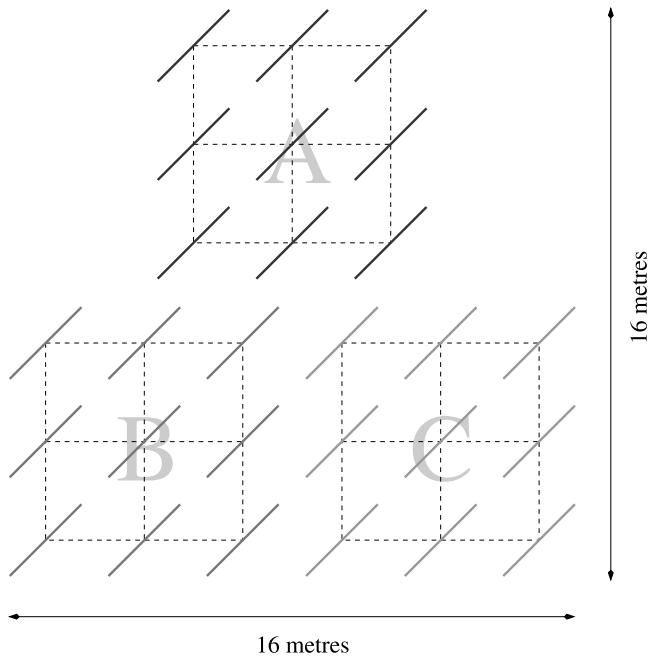


Figure 1. Plan view of antenna array. The groups labeled A, B, and C denote the antenna subgroups used for reception. The whole array was used for transmission.

[4] Dynamics also play a role in the spectrum of gravity waves generated by convection. At least three mechanisms, including mechanical oscillations, latent heat release and the flow over the top of the storm, are involved [see, e.g., *Beres et al.*, 2002, and references therein]. In their study, *Beres et al.* [2002] note the importance of tropospheric winds in controlling the strength and direction of waves generated by convection. Wind shears and associated wave refraction and critical-level interactions in the troposphere can alter the momentum flux entering the stratosphere.

[5] In order to study in detail the dynamics of the troposphere during DAWEX, a small VHF radar wind profiler was established at Pirlangimpi (Garden Point) on the northwestern part of Melville Island, adjacent to Apsley strait, the narrow body of water that separates Melville from Bathurst Island. A map showing the location of the radar and the relevant coordinates are given in the accompanying overview paper by Hamilton et al. (submitted manuscript, 2004). The radar allowed the basic flow in the lower and middle troposphere to be characterized during the IOPs, and the excellent height and time resolution enabled the wave field to be investigated on a diurnal basis.

[6] The paper is organized as follows. Section 2 describes the radar system and its calibration. Wind measurements are discussed in section 3, with descriptions of the mean winds observed during all IOPs and wave motions in IOP2. The results are discussed in section 4 with a comparison between profiler wave observations on 17 November and numerical model results.

2. Equipment and Calibration

[7] The VHF radar used in the DAWEX campaigns was similar to the small system described in the work of

Vincent et al. [1998]. This was designed to study tropospheric dynamics down to heights near 300 m in the boundary layer. However, the DAWEX radar was more powerful and used larger antennas for transmission and reception than the original system so that it had a better height coverage. The coverage was also improved by operating in a humid tropical environment since vertical gradients in humidity play an important role in determining radar reflectivities.

[8] The radar array was used for both transmission and reception. As shown in Figure 1, it consisted of three subgroups, each composed of nine three-element Yagi antennas arranged in a 3×3 matrix. Each Yagi was oriented at 45° to the major axes of the array so that the basic spacing was 0.5 wavelength. This ensured a compact arrangement and minimized sidelobes and associated ground clutter, which is important when receiving echoes from low altitudes. All antennas were phased to point vertically, with transmission on all 27 antennas in order to provide as narrow a beam as possible. The half-power-full-beamwidth (HPFB) of each subgroup was 32° , while the HPFB of the transmit antenna was 18° . Each subgroup was connected to its own receiver, and horizontal winds were measured using the spaced-antenna method [*Briggs*, 1984], while vertical velocities were computed from the Doppler shifts of the received signals.

[9] During DAWEX the radar operated in two modes. A low-level mode that used a 750 ns pulse to obtain 100 m height resolution over a height range between 300 m and 3.7 km and a high-level mode that used a 4 μ s length pulse to measure winds starting at 2 km with a height resolution of 600 m with data oversampled every 300 m. Table 1 summarizes the operating parameters used during the DAWEX campaigns.

[10] The power received by a VHF radar depends on the type of scattering or reflecting processes involved, which range from volume scatter to specular reflection. However, the common feature is a dependence on the gradient of radio refractive index, M [*Doviak and Zrnic*, 1993]. We made use of this dependence to check the radar height calibration. Correct range determination requires knowledge of signal delays through the radar system, including the cables connecting the antennas, which are not always easy to estimate accurately. As part of the calibration process, values of M^2 were derived from simultaneous high-resolution radiosonde observations made every 3 hours from Garden Point during the IOPs (see T. Tsuda et al., Characteristics of gravity waves with short vertical wavelengths observed with radiosonde and GPS occultation during DAWEX (Darwin Area

Table 1. VHF Profiler Operating Parameters

Operating Parameters	Low Mode	High Mode
PRF, Hz	20,000	8000
Pulse length, m	100	600
Range, km	0.3–3.8	2.0–10.0
Range sampling, m	100	300
Receiver bandwidth, kHz	404	253
Coherent integrations	1000	400
Number of samples	1100	1100
Acquisition length, s	55	55
Nyquist velocity, m s^{-1}	± 27.7	± 27.7

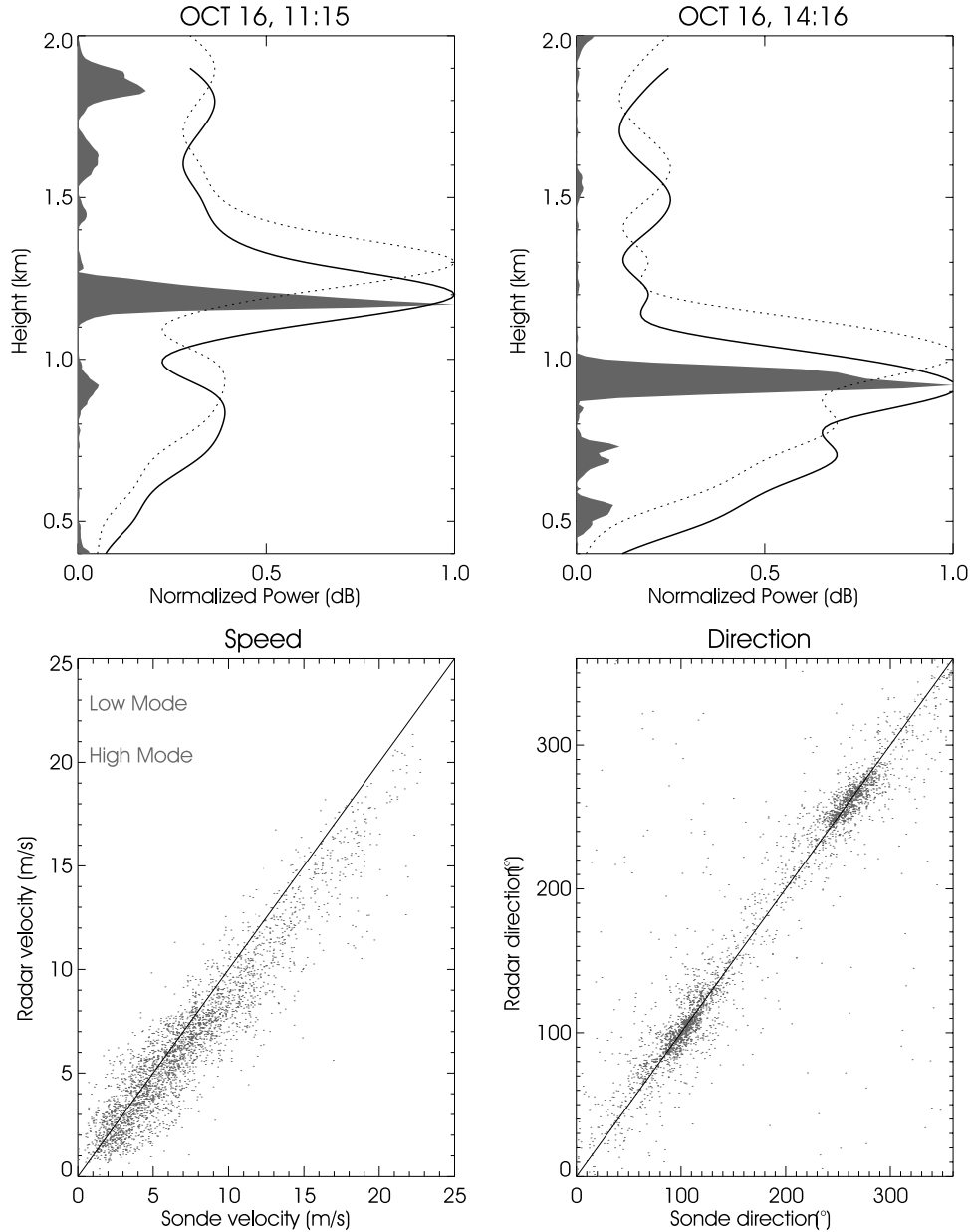


Figure 2. (top) Examples of comparisons of M^2 computed from radiosonde observations and radar power profiles (dotted) before and (solid) after moving downward by 100 m. (bottom) Comparisons of (left) speed and (right) direction of tropospheric winds measured by the VHF profiler and radiosonde observations at Garden Point during DAWEX.

Wave Experiment), submitted to Journal of Geophysical Research, 2004, for details).

[11] The refractive index gradient is given by

$$\begin{aligned}
 M &= \frac{\partial n}{\partial z} \\
 &= -77 \times 10^{-6} \frac{p}{T} \left(\frac{\partial \ln \theta}{\partial z} \right) \\
 &\quad \times \left[1 + \frac{15500q}{T} \left(1 - \frac{1}{2} \frac{\partial \ln q / \partial z}{\partial \ln \theta / \partial z} \right) \right], \quad (1)
 \end{aligned}$$

where n is the refractive index. Values of M^2 were computed from radiosonde profiles of temperature T , pressure p

(measured in hPa), potential temperature θ , and specific humidity q . The soundings had a 2-s time resolution, equivalent to an approximate 10 m height resolution. Comparisons of vertical profiles of echo strength and M^2 showed that the radar ranges were about 100 m too high (Figure 2). Accordingly, all measurements recorded by the radar have been shifted down by this amount. All heights mentioned from now on are corrected heights.

[12] After the radar ranges were corrected, the profiler winds were compared with the values determined from the radiosonde flights. Comparisons made over all campaigns are shown in Figure 2. There is good agreement between the two sets of observations, especially in direction. However,

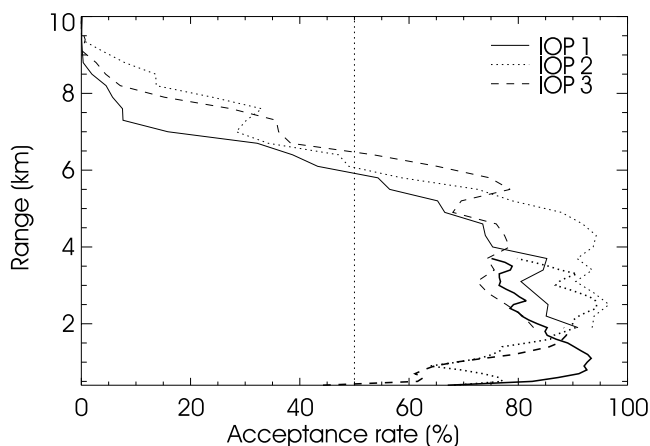


Figure 3. Percentage acceptance rate of horizontal winds derived from VHF profiler during the three DAWEX IOP campaigns.

in common with previous wind comparisons between spaced antenna radars and radiosondes, the speeds derived from the profiler underestimate the actual values by up to 9%.

[13] The system alternated between low and high mode every 1 min, so the nominal time resolution for each mode was 2 min. However, the actual time resolution achieved depended on the presence of suitable scattering irregularities. Figure 3 shows the percentage acceptance rate of horizontal wind measurements during the three IOP campaigns. The acceptance rate varied between 80 and 95% up to heights near 4 km and steadily decreased above this height, with the 50% acceptance rate occurring near 6 km.

As discussed later, there is also a diurnal variation in echo strengths and height coverage.

3. Observations

3.1. Mean Winds

[14] The profiler observations show that the mean winds changed systematically between the first campaign in October and the final campaign in December, as illustrated in Figure 4. In October the zonal wind averaged over the whole campaign is westward (easterly) at all heights, with a peak value of 6 m s^{-1} near 2 km. The meridional component is northward (southerly) above 2 km and weakly southward below this height.

[15] In November the westward zonal winds had increased in strength, peaking near 3 km altitude at 12 m s^{-1} , although at heights below 1 km the winds had reversed to weak eastward (westerly) winds. The meridional component was northward at all heights up to 8 km, with maximum values of 5 m s^{-1} . These conditions are typical of monsoon break period when Hector's are formed [Keenan *et al.*, 2000].

[16] By the time of the December IOP the zonal winds had reversed direction, becoming eastward (westerly) at all heights of observation, with mean values of about 5 m s^{-1} . This kind of flow is typical of the monsoon over northern Australia. The meridional winds show a weak shear, changing from a $1\text{--}2 \text{ m s}^{-1}$ near the ground to a weak southward flow of similar magnitude near 8 km.

[17] Examination of the mean winds during each IOP showed little evidence for any systematic variations with time. For reference, Hamilton *et al.* (submitted manuscript, 2004) provide a time-height plot of hourly average zonal winds during IOP2 derived from the profiler

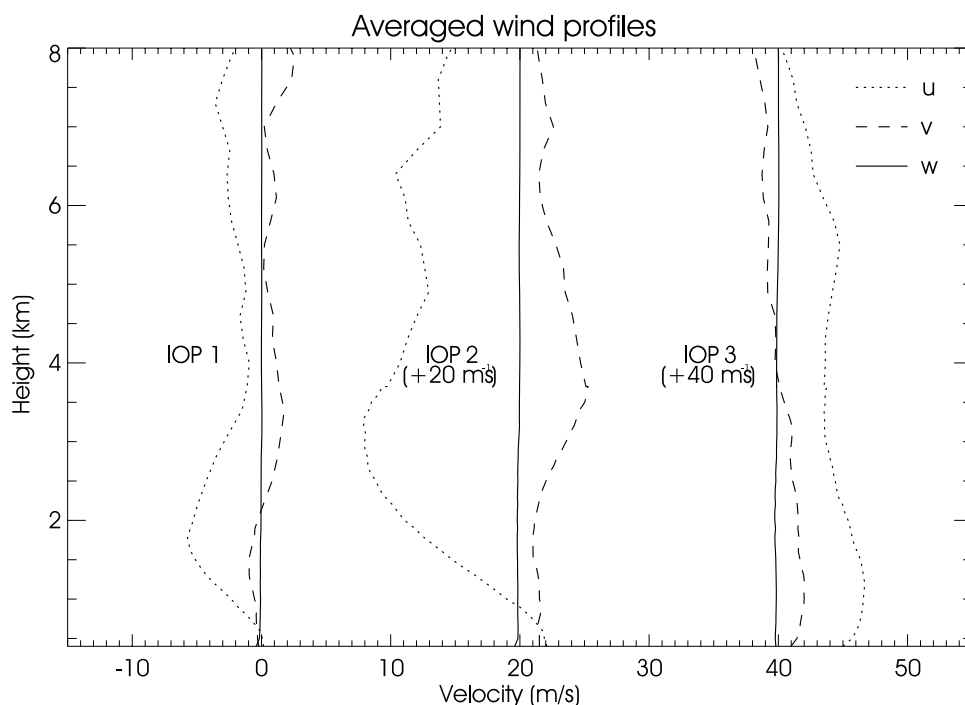


Figure 4. Vertical wind profiles of (dotted) mean zonal, (dashed) meridional, and (solid) vertical wind components in the lower troposphere during the intensive observation campaigns.

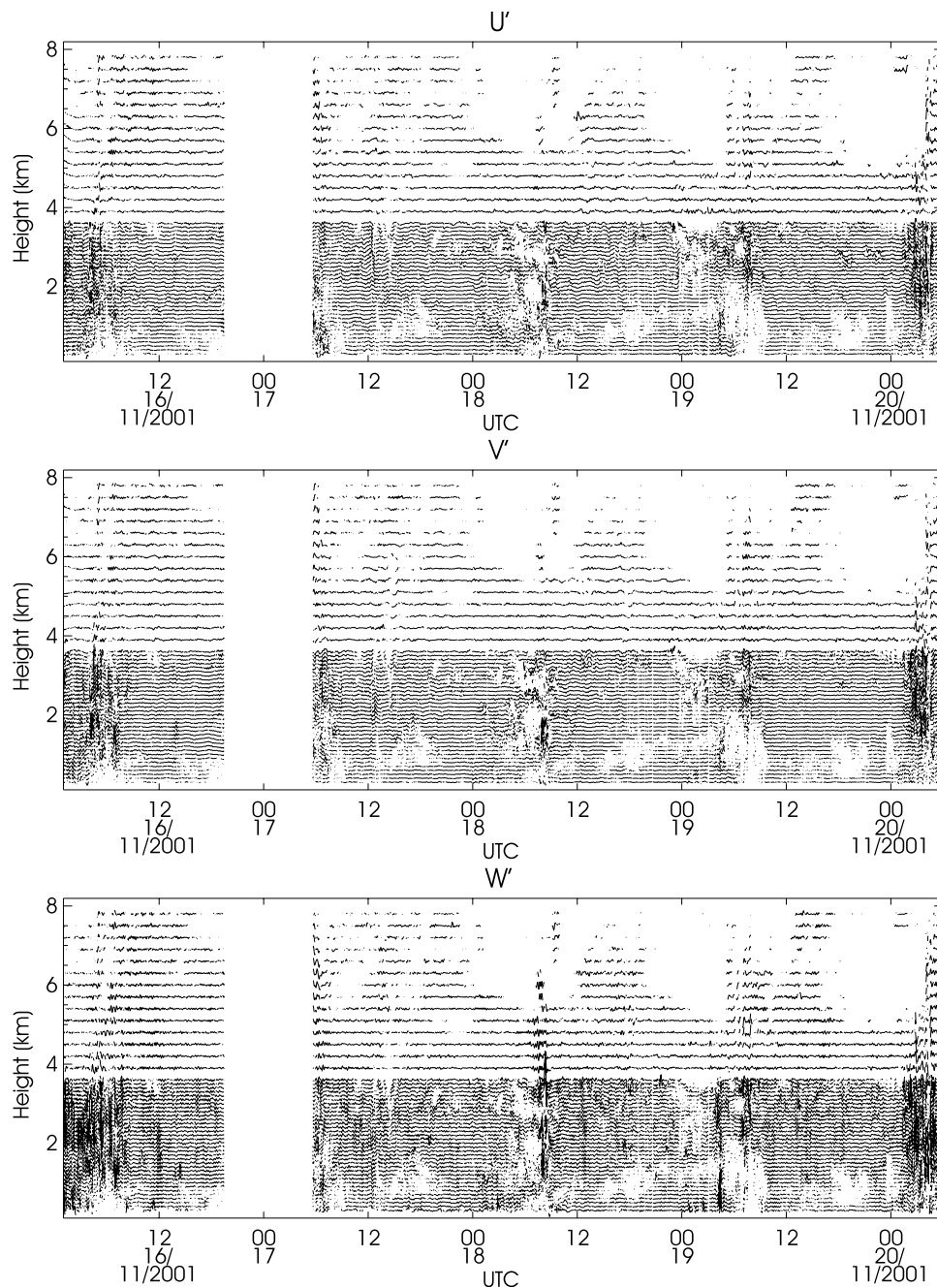


Figure 5. Stacked plots of (top) zonal, (middle) meridional, and (bottom) vertical wind components during the November campaign. The height resolution is 100 m up to 3.6 km and 300 m above that height. The time series are filtered between periods of 12 and 180 min.

observations. This shows that there is little significant diurnal variation of the winds. In summary, the mean horizontal winds observed by the profiler during each IOP were in good agreement with the general flow patterns observed over northern Australia, as discussed in the work of Hamilton et al. (submitted manuscript, 2004).

[18] Vertical velocities were measured from the Doppler shifts of the backscattered echoes. At all times the mean vertical velocities were very small and, on average, zero. Examination of the raw data did indicate short periods of

significant updrafts, with peak velocities of a few meters per second during strong convection.

3.2. Wave Observations

[19] As noted above, the effective wind sampling interval is greater than 2 min at each height owing to missing data. To provide time series of the winds, each wind component was averaged over 4 min intervals, and missing data were linearly interpolated over. In order to study variations that might be due to gravity waves generated by Hector and other convective storms in the vicinity of Darwin, the data

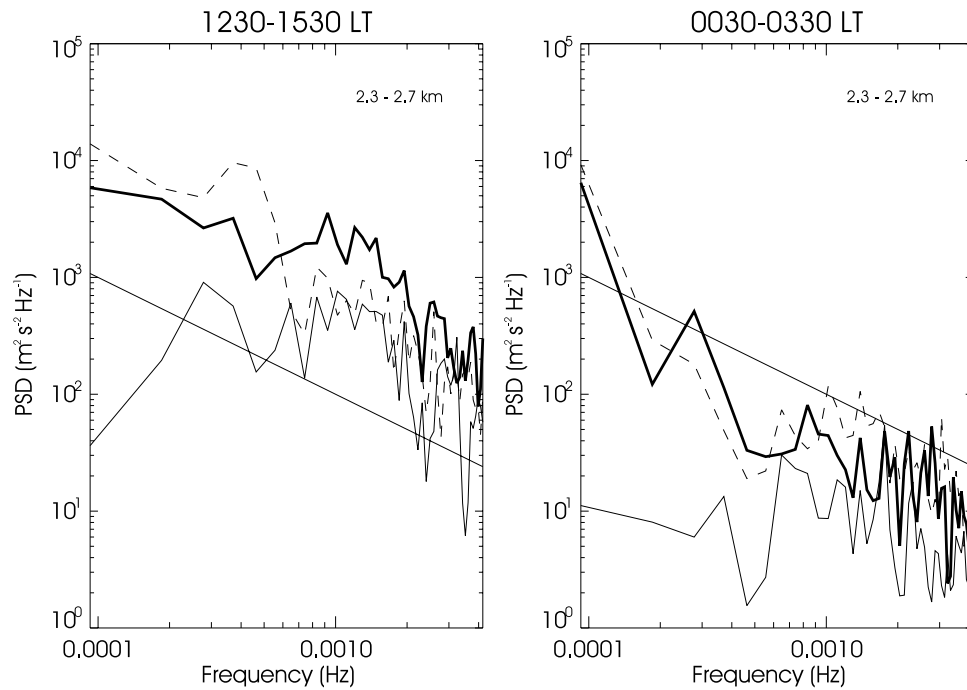


Figure 6. Frequency spectra for the (dark solid line) zonal, (dashed line) meridional, and (light solid line) vertical perturbation motions observed in the 2.3 and 2.7 km height region. The spectra are averaged over all days of observation in IOP2 for the time intervals shown. For reference, the straight line in each panel has a slope of $f^{-5/3}$.

at each height were filtered with a bandpass between 12 and 180 min. Time series of the filtered wind components are plotted in Figure 5 as a function of height. The data are plotted with a height spacing of 100 m up to 3.6 km, and then at a spacing of 300 m.

[20] Several features are evident in Figure 5. First, there is a strong diurnal modulation of height coverage. Winds are often measured up to heights near 8 km during periods between ~ 0600 and 1800 UT (1530 – 0330 LT). This change is due to increased reflectivities brought about by the uplift of water vapor into the middle troposphere by the afternoon convective storms. As shown by equation (1), the refractivity is a strong function of specific humidity q . Another factor in improving the height coverage is the increased levels of turbulence associated with the convection and the corresponding increase in strength of the scattering irregularities.

[21] The second feature is the absence of wind measurements at the lower heights during times when convection is strong. For example, for a period centered on 0600 UT (1530 LT) on 19 November, there is an absence of wind measurements up to heights near 2 km. There are two reasons for these gaps. Any convective cells passing over the radar produced strong small-scale variations in winds, causing spectral broadening of the echoes. Correspondingly, the correlation functions used in the spaced antenna full correlation analysis (FCA) are narrow, and the analysis often breaks down. The second reason for a lack of wind measurements was caused by the radar's location adjacent to Apsley strait. Radar backscatter from sea waves usually produces narrow spectral lines that are relatively easy to remove in the spectral domain before

the FCA is carried out. However, during convective storms, the strong winds produce enhanced sea surface roughness, which led to strong spectral broadening of the sea clutter. It was often impossible to distinguish the clutter part of the spectrum from the atmospheric component, which itself was broadened owing to the stronger turbulent motions. Under these conditions the wind analysis often broke down or produced spurious results.

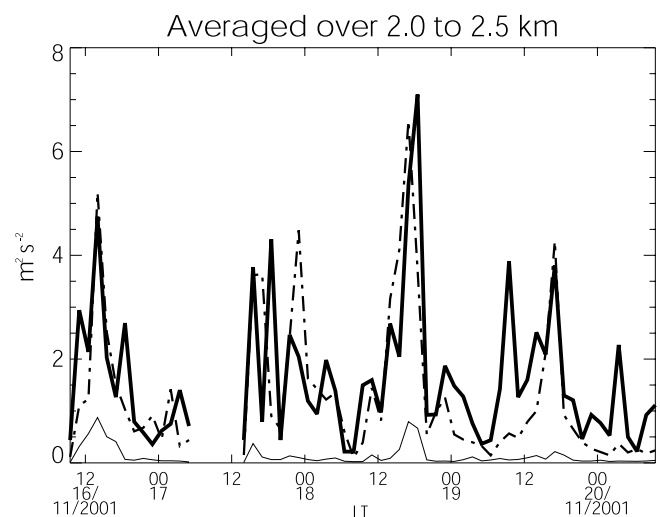


Figure 7. Mean square amplitudes of the (dark solid line) zonal, (dashed line) meridional, and (light solid line) vertical wind components in the 8-min to 3-hour period band observed between 2 and 2.5 km during IOP2.

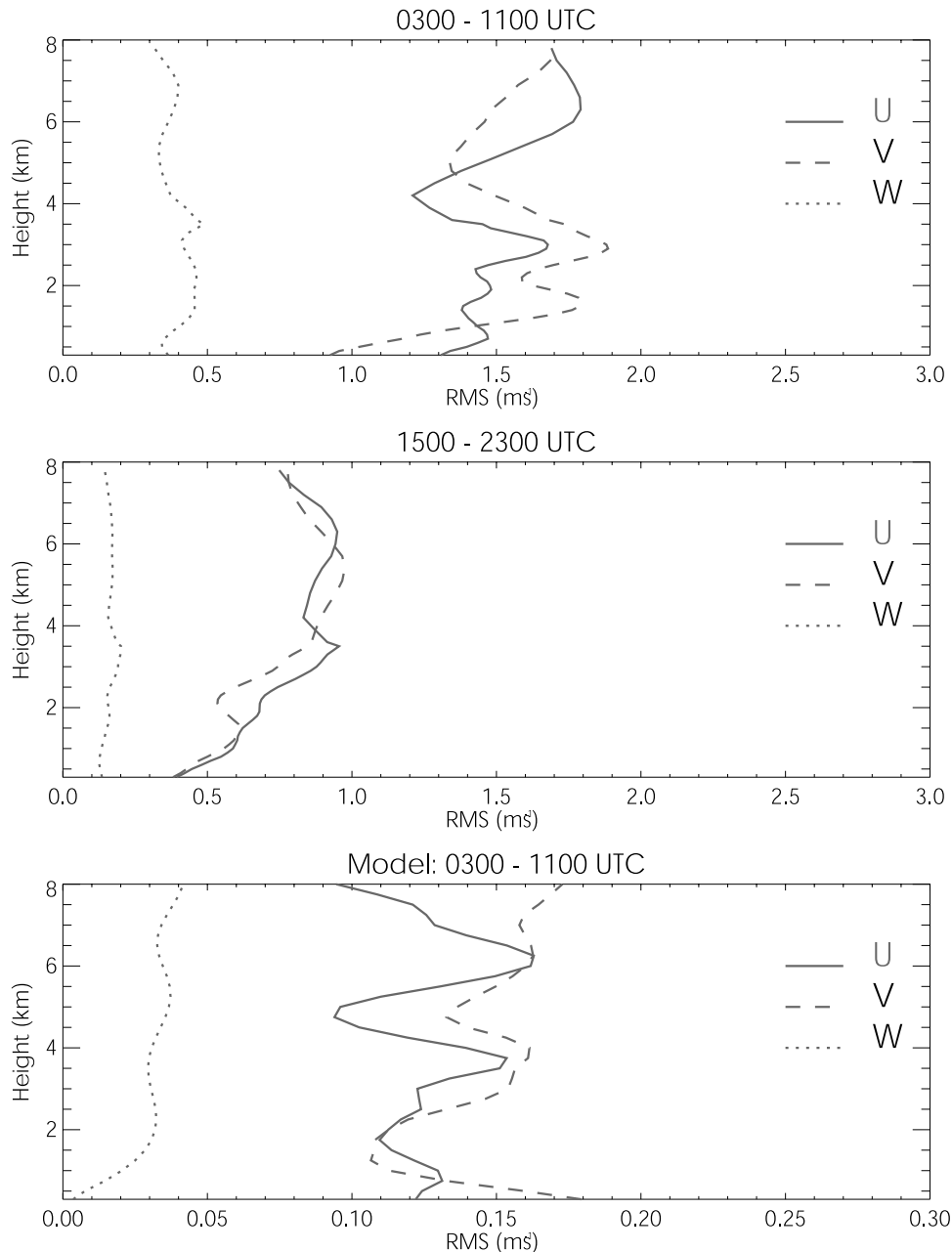


Figure 8. Height profiles of rms amplitudes for motions in the 12–180 min period range for the intervals (top) between 0300 and 1100 UT (between 1230 and 2030 LT) and (middle) between 1500 and 2300 UT (between 0030 and 0830 LT). (bottom) Gravity wave amplitudes derived from a numerical simulation for 0300–1100 UT, 17 November 2004 [Alexander *et al.*, 2004].

[22] Notwithstanding the complications in making wind measurements when strong convection was present, it is possible to determine gravity wave amplitudes. First, power spectral analyses were carried out for each wind component to study the distribution of wave energy as a function of frequency. In order to study the evolution of the spectra as a function of time, the spectra were computed in 3-hour time intervals, each overlapped by 1.5 hours. The number of degrees of freedom, and hence spectral reliability, was increased by averaging spectra together over a range of heights and for all days of observation. Figure 6 shows spectra computed for the 0300–0600 UT (1230–1530 LT)

and 1500–1800 UT (0030–0330 LT) intervals in the 2.3–2.7 height range. Each spectral estimate has a notional 50 degrees of freedom associated with it, although the use of 100 m radar pulses means that the observations made at adjacent range gates may not be fully independent.

[23] There is a clear difference in both the spectral shape and amplitudes between motion fields observed in the two intervals that are 12 hours apart. First, in the early afternoon interval, the spectral energy of all three wind components is 1–2 orders of magnitude larger than the values observed in the early morning interval. Second, the horizontal motions, and particularly the zonal (u') component, have a broad

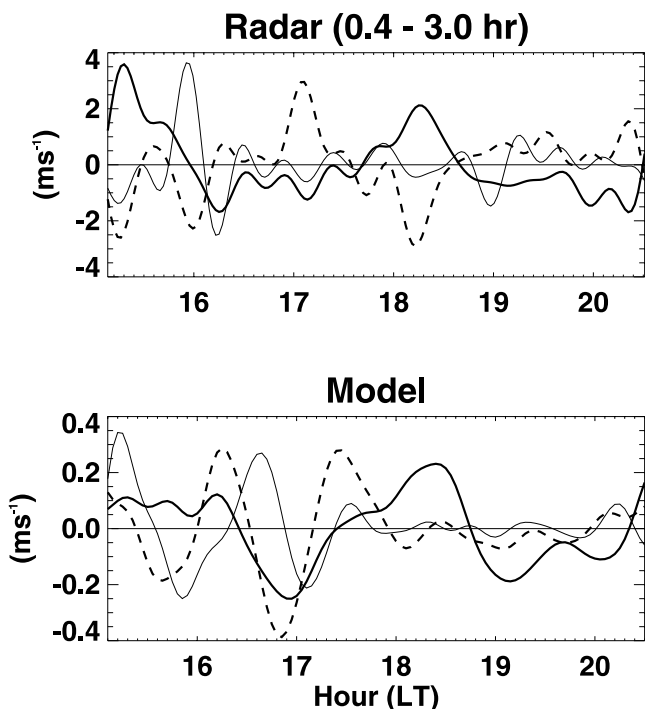


Figure 9. Comparison for a height of 2.5 km of (top) observed and (bottom) model wave amplitudes for the (dark solid line) zonal, (dashed line) meridional, and (light solid line) vertical wind components. Note that for ease of comparison, the vertical velocities have been increased by a factor of 4.

peak at frequencies between 2×10^{-3} and 1×10^{-3} Hz, i.e., at ground-based periods between ~ 8 and 17 min. This peak is even more evident when the spectra are plotted in area preserving form.

[24] It should be pointed out that differential vertical motions across the radar beam can appear as spurious horizontal motions in the spaced antenna analysis [Briggs, 1980] and can distort a spectrum of gravity wave motions [Rastogi *et al.*, 1996]. The effect is significant when the differential vertical motions have scales of the diameter of the of the area subtended by the radar beam, which at a height of 2–3 km is ~ 1 –1.5 km. It seems unlikely that gravity waves would have horizontal wavelengths as short as this.

[25] The area under each spectrum gives the mean square amplitude of the motions. Time series for IOP2 of the mean square amplitude of each wind component observed in the height range 2–2.5 km are provided in Figure 7. Results are plotted for 3-hour time intervals, overlapped by 1.5 hours. The figure brings out more clearly the strong diurnal cycle in activity evident in Figure 5. Peak rms values range between about 2 and 2.5 m s^{-1} for both u' and v' and between about 0.5 and 1 m s^{-1} for w' .

4. Discussion

[26] The results presented above need to be placed in context with respect to the meteorological conditions that pertained at the time in IOP2. Using C-pol radar reflec-

tivities as a guide, Hector-like storms appeared on the Tiwi Islands every afternoon between 15 and 19 November (Hamilton *et al.*, submitted manuscript, 2004). Typically, they had maximum development between 0330 and 0600 UT (between 1300 and 1530 LT). In general, the storm cells passed either to the south or north of Garden Point by distances of up to 20–40 km (see, e.g., Hamilton *et al.*, submitted manuscript, 2004, Figure 10). However, on 16 November a strong convective storm passed almost over Garden Point at about 0430 UT (1400 LT) and again on 17 November at about 0410 UT (1340 LT). In evening hours, squall lines appeared over continental Australia, usually being quite intense at about 1200 UT (2130 LT) and traveled northwestward toward the Tiwi Islands.

[27] On the basis of the C-Pol reflectivities the Hector on the 18 November was the strongest storm of IOP2 (P. T. May, private Communication, 2004), which correlates with the strongest peak in variances (Figure 7). It is not easy to assess how much of the wind fluctuations measured by the VHF profiler can be ascribed to convective motions and how much due to waves. The proximity of the storm to the radar on the 18 November means that the motions could be due to a combination of convective motions and wave motions as the storm passed just to the north of the radar on that date. However, the fact that storms passed some 20 km or more from the profiler on other days suggest that wave motions are responsible for peak variances of $12 \text{ m}^2 \text{ s}^{-2}$ in horizontal motions and 0.5 – $1 \text{ m}^2 \text{ s}^{-2}$ in the vertical motions.

[28] The frequency spectra shown in Figure 6 suggest that much of the wave energy is concentrated at ground-based periods between 8 and 17 min, which is close to the buoyancy frequency of 9–10 min in the lower troposphere during IOP2. Various numerical modeling studies that use realistic environments for the initiation and development of Hectors show dominant gravity waves with wavelengths of 15–25 km and intrinsic periods between 15 and 20 min [Piani *et al.*, 2000; Lane *et al.*, 2001; Lane and Reeder, 2001]. The rather monochromatic wave fields that appeared above the tropopause in these models were ascribed by Lane and Reeder [2001] to convective overshoot of air parcels and oscillations around the level of neutral buoyancy.

[29] Alexander *et al.* [2004] in an accompanying paper describe a numerical simulation of gravity wave generation by convection during DAWEX. They used C-Pol weather radar reflectivities (see Hamilton *et al.*, submitted manuscript, 2004 for details) to delineate the temporal and geographic variability of gravity wave forcing by latent heat release during convection. The model, which is uses a $400 \times 400 \text{ km}$ domain centered on the C-Pol radar, has a 2-km resolution in the horizontal and 0.25 km in the vertical. Alexander *et al.* [2004] focus on a 7-hour period on 17 November 2001 from 0300 to 0950 UT (1230 to 1920 LT). The conditions on this day are typical of all days during IOP2, i.e., there were Hectors in the afternoon and continental squall lines in the evening. In the area covered by the C-Pol radar the maximum volumetric heating rates peaked at about 0430 and 0830 UT.

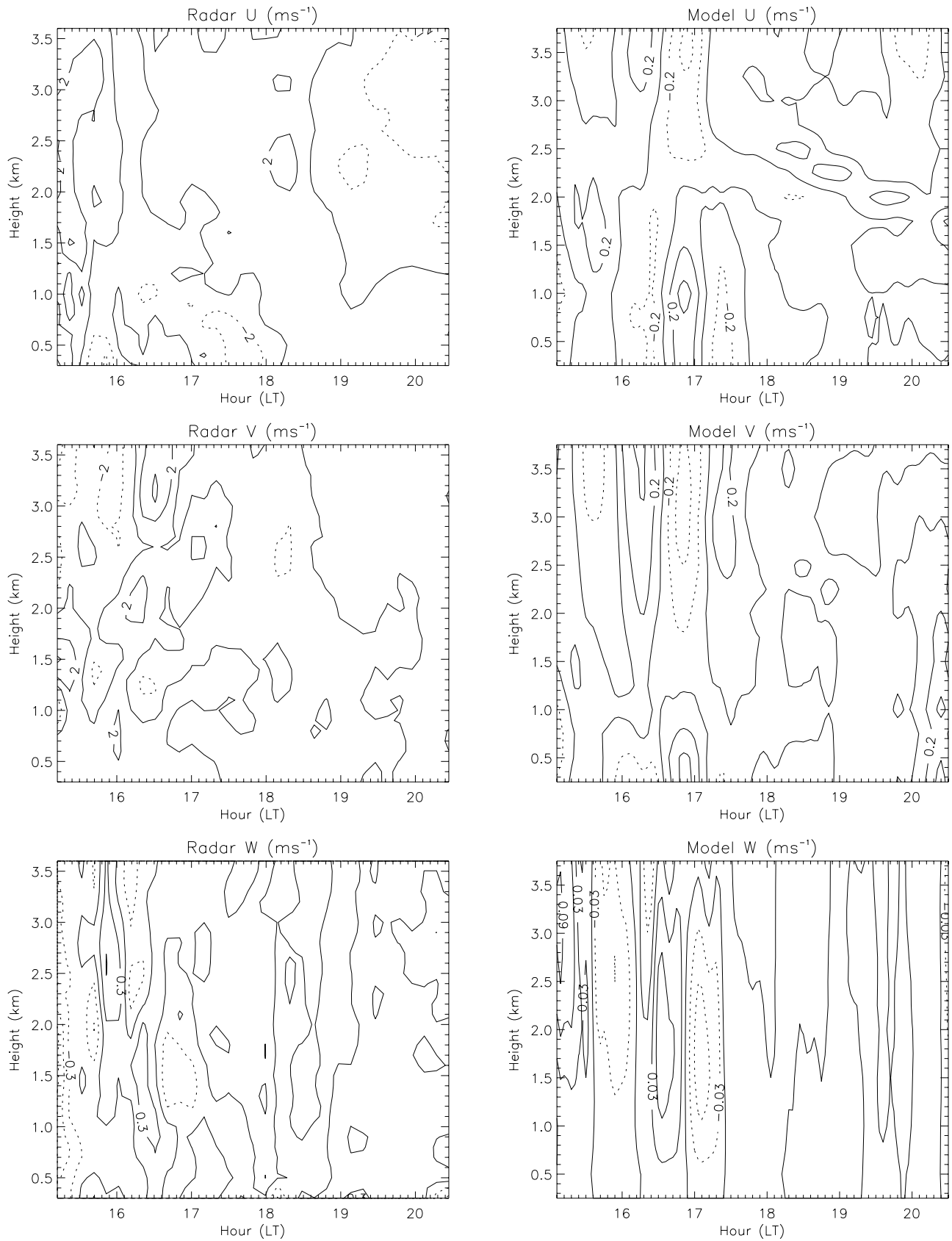


Figure 10. Time-height cross sections of perturbation amplitudes in the 20–180 min range from (left) profiler and (right) model. The top panels show u' , middle panels show v' , and bottom panels show w' .

[30] Figure 8 shows height variations of wave amplitudes derived for 17 November. In order to compare in more detail with results derived from a numerical model (see below), the data were divided into two intervals, one centered on the most active period between 0300 and 1100 UT (between 1230 and 2030 LT) and the other centered on the early morning hours (1500–2300 UT or 2330–0830 LT), when convection was not strong. During the active period in midafternoon (local time), rms amplitudes were about 1.5 m s^{-1} for both horizontal wind components, while the value for the vertical component was $\sim 0.4 \text{ m s}^{-1}$. Both u' and v' show some height structure, while w' is almost constant with height. Amplitudes during the early morning hours are 2–3 times smaller for all components than in the afternoon period and the height profiles are smoother.

[31] The tropospheric perturbations in the model at the model grid point closest to the Garden Point profiler can be compared to the radar wind values. Model results for the 0300–1100 UT time interval are shown in the bottom panel of Figure 8. Amplitudes of the horizontal perturbation motions lie in the range $0.1\text{--}0.16 \text{ m s}^{-1}$, while the vertical motion amplitudes are about 0.03 m s^{-1} . Interestingly, the height structure of the model and observed winds are rather similar. However, the model values are approximately a factor of 10 smaller than the profiler measurements, an issue that is discussed further below.

[32] Figure 9 compares time series of the observed and model winds for a height of 2.5 km. The data have been filtered to remove periods shorter than 24 min and longer than 3 hours. Despite the filtering, the observations show distinct short period oscillations that are not evident in the model results. This difference is likely associated with short horizontal-scale motions in the data that are either advected or propagate over the radar site. The model resolution is only 2 km, and the numerical dissipation effectively damps horizontal-scale fluctuations at scales 10 km and shorter.

[33] What is particularly apparent, however, is the similarity between the model and observed fluctuations. These similarities are especially evident in the u' components, which show very similar phases, evolution with time, and are dominated by ~ 2 -hour period waves. The v' components, however, show stronger oscillations at periods near 1 hour in the first part of the record, but which are absent in the last part from about 0830 UT onward. The vertical velocity components similarly have larger amplitudes in the interval before 1800 LT. Again, it is noteworthy that the observed amplitudes are some 5–10 times larger than the model values.

[34] Perturbations as a function of height and time are displayed in Figure 10. The observations were filtered to include fluctuations with periods 20 min to 3 hours, and the model for fluctuations shorter than 3 hours. Clearly, there are some differences between the observations and model results owing to the somewhat different spectrum of oscillations that are present in each data set (as noted above the model effectively filters out higher frequency motions). The broader bandwidth of the radar results leads to less coherence in the motions with height and time. Despite the differences, there are some remarkably similar features in both the model and the data. First is the time evolution, with much larger amplitude, vertically

coherent structures that appear only in the first portion of the time record, and which are absent in both data and model at later times. There is also a very similar short vertical-scale feature in the second half of the time period in the zonal wind perturbations that shows downward phase propagation. This may be a signature of a zonally propagating wave that appears at both the same time and place in both the data and the model. The meridional and vertical motions tend to show more vertical structure, although there is evidence of vertical phase tilt in the observed vertical component at about 0630 UT.

[35] Despite the similarities the wave amplitudes in the model are roughly 10 times smaller than the observations. At face value this difference would suggest that the model input heating and output wave amplitudes should be scaled upwards by about a factor of 10. The problem is that the exact conversion between the latent heating and wave generation is unknown.

5. Summary and Conclusions

[36] The VHF profiler observations presented here allowed us to explore gravity wave variability in the lower troposphere in the vicinity of intense deep convective storms (Hectors) over the Tiwi Islands in northern Australia. During the November 2001 campaign for DAWEX a strong diurnal cycle in wave activity was observed, with peak wave amplitudes reached in midafternoon. For waves with periods in the 8–180 min period range, an approximately 10:1 ratio between the largest and smallest variances is found. Oscillations with ground-based periods between 8 and 17 min are especially prominent in the early afternoon measurements. In general, during the November campaign, areas of strongest convection passed either to the north or south by distances ranging from 10 to 30 km, so these observations represent the “near-field” response to the convection.

[37] A case study for 17 November 2001 compares radar observations with results from a numerical model using weather radar reflectivities to help simulate gravity wave forcing due to latent heat release in convection [Alexander *et al.*, 2004]. There are significant similarities between the model and observed fluctuations, which provide encouragement to carry out further comparisons. An important issue requiring resolution is the “calibration” of the model wave amplitudes. One approach this issue is to exploit the ability of VHF boundary layer profilers to measure raindrop size distributions with good time and height resolution down to heights near the surface [Lucas *et al.*, 2004]. Using a VHF profiler in conjunction with cloud and weather radars, it would be possible to investigate convective cloud microphysics in more detail. This would provide better understanding of the relationship between weather radar reflectivities and latent heat release, in turn providing better specifications of latent heat release for model simulations of gravity waves.

[38] **Acknowledgments.** We gratefully acknowledge the Tiwi Land Council for their support and permission to operate the profiler at Pirlangimpi. Helpful discussions with P. T. May are also appreciated. This work was supported by Australian Research Council grants A69802414 and X00001692.

References

- Alexander, M. J., P. T. May, and J. H. Beres (2004), Gravity waves generated by convection in the Darwin area during the Darwin Area Wave Experiment, *J. Geophys. Res.*, *109*, D20S04, doi:10.1029/2004JD004729, in press.
- Beres, J. H., M. J. Alexander, and J. R. Holton (2002), Effects of tropospheric wind shear on the spectrum of convectively generated gravity waves, *J. Atmos. Sci.*, *59*, 1805–1824.
- Briggs, B. H. (1980), Radar observations of atmospheric winds and turbulence: A comparison of techniques, *J. Atmos. Terr. Phys.*, *42*, 823–833.
- Briggs, B. H. (1984), The analysis of spaced sensor records by correlation techniques, in *Handbook for MAP, 13*, edited by R. A. Vincent, pp. 166–186, SCOSTEP Secretariat, Urbana, Ill.
- Doviak, R. J., and D. S. Zrnic (1993), *Doppler Radar and Weather Observations*, 2nd ed., Academic, San Diego, Calif.
- Hamilton, K., and R. A. Vincent (2000), Experiment will examine gravity waves in the middle atmosphere, *Eos Trans. AGU*, *81*, 517.
- Keenan, T., et al. (2000), The Maritime Continent Thunderstorm Experiment (MCTEX): Overview and some results, *Bull. Am. Meteorol. Soc.*, *81*, 2433–2455.
- Lane, T. P., and M. J. Reeder (2001), Convectively generated gravity waves and their effect on the cloud environment, *J. Atmos. Sci.*, *58*, 2427–2440.
- Lane, T. P., M. J. Reeder, and T. L. Clarke (2001), Numerical modelling of gravity wave generation by deep tropical convection, *J. Atmos. Sci.*, *58*, 1249–1274.
- Lucas, C., A. D. MacKinnon, R. A. Vincent, and P. T. May (2004), Rain-drop size distribution retrievals from a VHF boundary layer profiler, *J. Atmos. Oceanic Technol.*, *21*, 45–60.
- Piani, C., D. Durran, M. J. Alexander, and J. R. Holton (2000), A numerical study of three-dimensional gravity waves triggered by deep tropical convection and their role in the dynamics of the QBO, *J. Atmos. Sci.*, *57*, 3689–3702.
- Rastogi, P. K., E. Kudeki, and F. Surucu (1996), Distortion of gravity wave spectra of horizontal winds measured in atmospheric radar experiments, *Radio Sci.*, *31*, 105–118.
- Vincent, R. A., S. Dullaway, A. MacKinnon, I. M. Reid, F. Zink, P. T. May, and B. H. Johnson (1998), A VHF boundary layer radar: First results, *Radio Sci.*, *33*, 845–860.
-
- M. J. Alexander, Colorado Research Associates, 3380 Mitchell lane, Boulder, CO 80301, USA. (alexand@cora.nwra.com)
- A. MacKinnon, I. M. Reid, and R. A. Vincent, Department of Physics, School of Chemistry and Physics, University of Adelaide, Adelaide 5005, South Australia. (andrew.mackinnon@adelaide.edu.au; iain.reid@adelaide.edu.au; robert.vincent@adelaide.edu.au)